Article

Single-Layered Paper-Based Microfluidic Devices Made by Paint-Spraying Technique with Great Barrier Resistance for Colorimetric Assays

Beixi Nie,[#,a] Shaoyu Zhao,[#,a] Muhan Deng,[#,a] Peng Yu, [⬤]*,a *Yi Yang,[a] Weixin Lei[a] and Lu Yin[a]*

[a]School of Materials Science and Engineering, Xiangtan University, 411105 Xiangtan, China

The single-layered paint-spraying paper based microfluidic devices (sp-µPADs) have been for the first time integrated with the colorimetric assay. The polymethyl methacrylate (PMMA) board was applied as the mask instead of the iron mask, reducing the power requirement of the cutting machine. The paint was sprayed into the paper, which blocked the pores of the paper and constructed the hydrophobic barrier on the paper. The paint barrier was highly resistant to the various kind of chemicals and the minimum channel dimensions was 1.4 mm. By using the PMMA masks with different designs, the sp-µPADs with different designs have been fabricated and successfully applied to the single analyte assay of iron or bovine serum albumin (BSA) and the simultaneous assay of copper and nickel. Moreover, the feasibility of the multiplexed assay of eight analytes was also demonstrated. The analytical performances indicated that the fabricated sp-µPADs offered a promising platform in the colorimetric assays of either single or multiple analytes.

Keywords: microfluidics, paper-based devices, paint spraying, colorimetry

Introduction

Microfluidic paper-based devices (µPADs) have become an alternative point-of-care (POC) analytical tool since the work reported by Whitesides and co-workers in 2007.[1] The µPADs possess the advantages of simplicity, portability, miniaturization, in-field capability and low-cost with a comparison to the traditional measurement methods.[2] In recent years, µPADs have been integrated with various kind of analytical techniques, such as mass spectrometry (MS),[3,4] electrochemistry,[5,6] surface plasmon resonance (SPR),[7,8] colorimety,[9-11] fluorometry,[12-14] electrophoresis,[15] chromatography,[16] and chemiluminescence.[17,18] Among these techniques, the colorimetry integrated with µPADs was most attractive, in which color or light intensity variations are monitored by a mobile phone camera or a color image scanner, and analyzed by an open source image processing program.[19] The colorimetric µPADs have been used for rapid qualitative and quantitative analysis in various fields such as biochemical analysis, food safety, environmental monitoring, and point-of-care clinical diagnostics.[20-24]

One of the major challenges in the fabrication of µPADs is to pattern the hydrophilic paper with hydrophobic materials to define a reaction zone for the analyte measurement.[25]

Up to now, many techniques have been developed for the fabrication of µPADs. The photolithography technique, while expensive, produces devices with high resolution.[26] This method requires the usage of the clean room facilities including UV light sources, expensive photoresists, and oxygen plasma. Polydimethylsiloxane (PDMS) plotting,[27] screen-printing,[28] wax-printing,[29] ink-jet printing[30] and laser cutting[31] need the specialized instruments and the accompanying consumables. Other groups[32-34] have developed some instrumental-free techniques including stamping and drawing with permanent marker pen or eyeliner pencil. However, up-scaling such a production technique has been proven to be difficult. Therefore, it is highly desirable to develop a new low-cost approach, allowing for the rapid prototyping and the large scale manufacture of µPADs.

Spraying technology has become a new prototyping process for the µPADs manufacture emerging in recent years. Compared with the classic wax-printing technique, the spraying technology avoided the printing process, representing a major breakthrough in the µPADs manufacture.[35] Coltro and co-workers[36] described a glue-spraying technique for fabricating the µPADs and the hydrophobic barriers were created by the available scholar glue. In order to produce high resistance barrier, the paper coated with glue was dried at 130 ℃ for 60 min and then exposed under a halogen spotlight for 30 min.

This tedious heating step significantly increased the time for the µPADs fabrication. Chailapakul and co-workers[37] proposed a spraying method with paint for the µPADs fabrication. The paint is water resistant and good adhesive to various kinds of materials, and does not require the complex drying step.[38] The patterned iron mask was used to confine the barrier, proposing a higher requirement for cutting machines and undoubtedly increasing the fabrication cost. Additionally, the paint spraying µPADs developed by Chailapakul and co-workers[37] was applied for the electrochemical detection of Ni[II]. So far, no work has been reported on the colorimetric detection of one or more analytes with the paint spraying µPADs.

In this work, the single-layered paint-spraying µPADs (sp-µPADs) were integrated with the colorimetric method for the assays of one or more analytes. The patterned polymethyl methacrylate (PMMA) boards were used as the mask for the fabrication of sp-µPADs, which is cheaper than the iron mask. Spray paint was utilized to manufacture the two-dimensional channels in the filter paper. At first, the filter paper was masked with the patterned PMMA boards and then sprayed with the paint. After that, the painted filter paper was dried in an oven. Both the simple and complex fluidic patterns were successfully fabricated by the paint spraying prototyping process. The barrier resistance and the smallest channel size were investigated. Moreover, the validation of the sp-µPADs was demonstrated by detecting one or more analytes based on the color intensity analysis or the distance analysis.

Experimental

Chemicals and equipments

Whatman filter paper No. 1 was used for sp-µPADs fabrication, which was bought from Whatman International Ltd. (Maidstone, England). Spray paint with a volume of 400 mL *per* can (blue color or yellow color) was purchased from the local automotive products shop for constructing the channels. The design of the mask was drawn by the software of ZWCAD.[39] The polymethyl methacrylate (PMMA) board (1 mm in thickness) was cut according to the design by a local laser cutting shop. The binder clips with a width of 19 mm were applied to fix the position of the PMMA boards on the filter paper. Bovine serum albumin (BSA), sodium lactate, tetrabromophenol blue (TBPB), chitosan with a viscosity of 400 mPa s, 3,3',5,5'-tetramethylbenzidine (TMB), the universal indicator, glucose oxidase (GOx) from *Aspergillus niger* (> 180 U mg^{-1}) and peroxidase from horseradish (HRP, > 200 units mg^{-1}) were provided by Aladdin-Reagent

Company (Shanghai, China). Lactate oxidase (LOx) from *Aerococcus viridans* was bought from Sigma-Aldrich (Shanghai, China). Fe(NO$_3$)$_3$•9H$_2$O, 1,10-phenanthroline monohydrate (phen), ascorbic acid, glucose, potassium thiocyanate, sodium nitrite, citric acid, ethanol, acetic acid, sulfanilamide, *N*-(1-naphthyl) ethylenediamine dihydrochloride (NED), ethylenediaminetetraacetic acid disodium salt (EDTA), sodium diethyldithiocarbamate (DDTC), dimethylglyoxime, tris base, cupric nitrate, nickel nitrate, and other chemicals were purchased from Sinopharm Chemical Reagent Co., Ltd. (Shanghai, China). The deionized water was prepared by a Milli-Q system (Bedford, USA). The pictures of the sp-µPADs were obtained by a cellular phone (Huawei Nova, Huawei Technologies Co., Ltd, Shenzhen, China) in a photography box with a size of 40 × 40 × 40 cm. The photography box was bought from Shijiazhuang Ruying Film and Television Equipment Sales Co., Ltd. in Shijiazhuang, China and equipped with 84 LED light beads inside. When taking pictures, the cell phone was placed on the photo window at the top of the photography box, and the vertical distance from the prepared µPADs was 8 cm. The color intensity in the different color channels (i.e., red (R), green (G) and blue (B) channels) were measured by the ImageJ software.[40] The purified drinking water produced by China Resources C'estbon Beverage Co., Ltd. in Shenzhen, China was employed as the complex sample for the recovery experiment.

sp-µPADs fabricated using a two-step paint spraying prototyping process

The schematic representation of the two-step paint spraying prototyping process for fabricating the device for the microzone assay was presented in Figure 1. One piece of filter paper was put in between two PMMA masks. The whole device was spray-painted for the first time. The filter paper was then taken out and heated at 60 °C for 10 min. After that, the two patterned acrylic plates were rotated by 90 degrees and the dried filter paper was put in the middle of the two patterned acrylic plates. Then, the whole device was spray-painted for the second time. The filter paper was then taken out and dried again as mentioned above. A photograph of the actual developed µPAD was provided in Figure 1 and the channel's pattern of the sp-µPADs can be easily changed by changing the mask with different designs.

The microzone assay of iron

Iron is a necessary nutrient to maintain the body growth and development.[41] Iron deficiency or overload could cause a bad influence on human health.[42] Thus, iron was detected
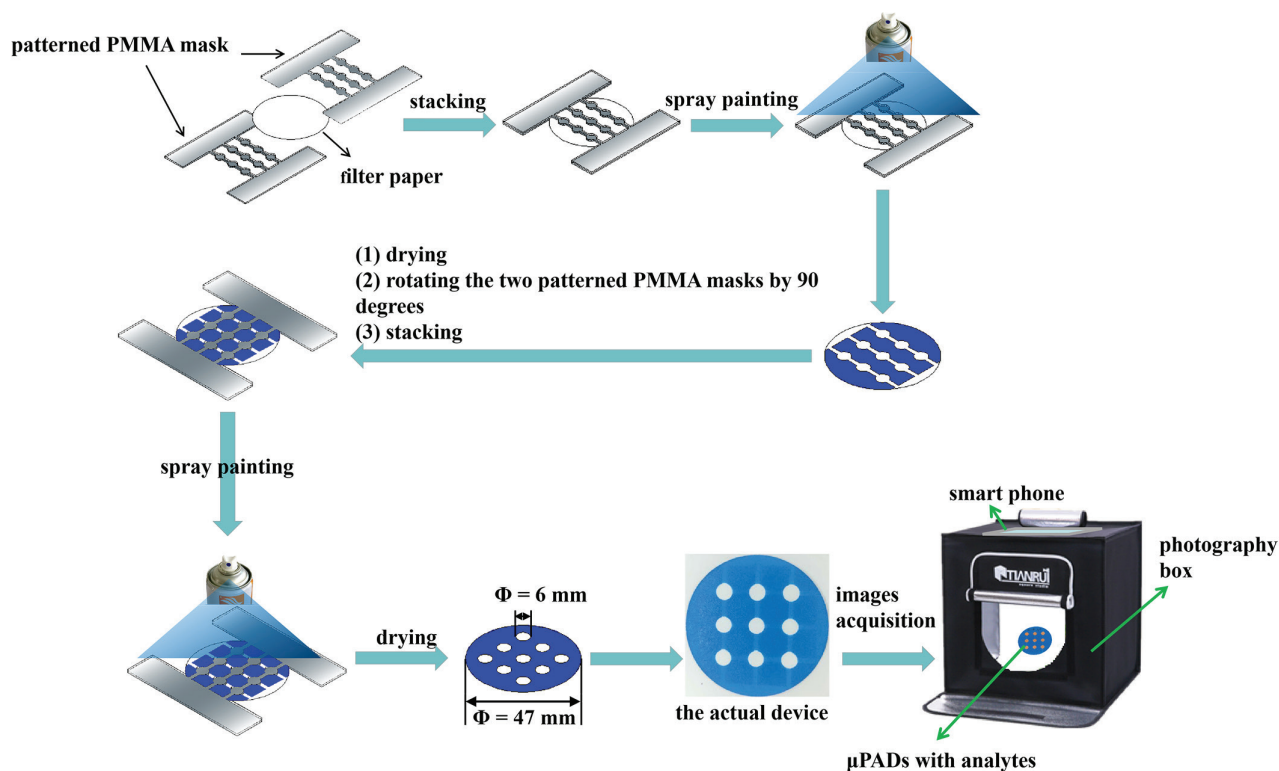
Figure 1. The schematic representation of the two-step paint spraying prototyping process for fabricating the device.

to investigate the application value of the sp-μPADs. The reagent for iron assay was prepared by adding 100 mmol L^{-1} phen, 2% (m/m) ascorbic acid in sodium acetate buffer (20 mmol L^{-1}, pH 4.6), using 95/5% (v/v) ethanol/water as the solvent. Then the reagent (2.5 μL) was pipetted into the microzone and dried at room temperature (RT) for 6 min. To generate a standard curve, the freshly prepared iron standards (2.5 μL) and the blank (ultrapure water) (2.5 μL) were added into the microzones of the μPAD. The pictures of the sp-μPADs were captured by a cell phone and the color intensities in different channels were analyzed by the ImageJ software.[40]

The multiplexed assay of eight analytes

The eight analytes including BSA, glucose, nitrite, thiocyanate, lactate, pH, copper and nickel were used for the multiplexed assay in this work. For BSA assay, 0.5 μL of the reagents including citric acid (250 mmol L^{-1}) and TBPB (3 mmol L^{-1}) in 95% (v/v) ethanol were pipetted into the outer circular assay zone.[43] For the assays of glucose and lactate, 0.5 μL of chitosan (0.5% m/v) in acetic acid (2% v/v) was pipetted into the corresponding assay zones. The enzyme solutions in PBS (100 mmol L^{-1}, pH 6.0) were composed of GOx (120 U mL^{-1}) and HRP (30 U mL^{-1}) for glucose assay and LOx (40 U mL^{-1}) and HRP (300 U mL^{-1}) for lactate assay, respectively. 0.5 μL of TMB solution

(15 mmol L^{-1}) was then pipetted into the assay zones.[44,45] For nitrite assay, the Griess reagent was composed of NED (10 mmol L^{-1}), sulfanilamide (50 mmol L^{-1}), and citric acid (330 mmol L^{-1}). 0.5 μL of the Griess reagent was added into the assay zone.[44] For thiocyanate assay, 0.5 μL of the solution containing 600 mmol L^{-1} Fe^{III} was added into the outer circular assay zone.[33] For pH assay, 0.5 μL of the universal indicator were pipetted into the outer circular assay zone.[46] For Cu^{II} assay, 0.5 μL of the solution containing 150 mmol L^{-1} EDTA and 5 mmol L^{-1} DDTC (pH 7.6) was pipetted into the outer circular assay zone.[47] For nickel(II) assay, 0.5 μL of the sensing solution composed of dimethylglyoxime (50 mmol L^{-1}) and tris base (50 mmol L^{-1}) in 95/5% ethanol/H$_2$O solvent was pipetted into the outer circular assay zone.[48] All these reagents were allowed to dry at RT for 10 min. Then, the model mixture containing the eight analytes (15 μL) was added to the circular zone in the center. After 10 min of reaction, the photo of the flower-shaped μPADs were taken using a smartphone.

Results and Discussion

Characterization of the fabricated sp-μPADs

The technical challenge in the sp-μPADs fabrication is how to control fluid flow in the channels.[49] In order to

achieve this goal, it is critical to construct the clear boundary to distinguish the hydrophilic area and the hydrophobic area. First, the hydrophobic property of the paint barrier was investigated. The water droplet was dropped on the surface of the sp-µPADs and the picture was shown in Figure 2A. The contact angle with water was 134°, indicating that the area deposited by paint exhibits hydrophobicity. The reason is that the paint blocked the pores in the filter paper, forming an hydrophobic interface on the surface of the paper. For the fabrication of device, it is critical to make sure that the paint fully penetrates into the filter paper. The fabricated µPAD was cut along the red dotted line and the cross section was observed by an optical microscope. It is clearly shown that the paint fully penetrates into the filter paper in the hydrophobic area and there is a well-defined boundary between the hydrophobic area and the hydrophilic area (Figure 2B). The manufacturing cost of a single device (including the cost of PMMA masks and laser cutting, filter paper, paint) is ca. US$ 0.17, manifesting the low cost of the paint spraying method. The channel size was calibrated and the results were presented in Figure 2C. The fabricated device for the channel size calibration possessed 12 radiating channels with the width ranging from 0.1 to 2 mm. It is noted that the smallest channel which was able to be filled in the entire length of the channel with red food dye, was revealed to be 1.4 mm with a designed width of 1.5 mm.

Investigation of the barrier resistance

The resistance when exposed to the various kinds of chemicals has been demonstrated. The paint with yellow color were used for the fabrication of the distance-based sp-µPADs to get a clear barrier view. The sp-µPADs used for this experiment included a circular zone for sample introduction with a radius of 4 mm and a channel with a width of 2 mm, whose size was marked in the Figure 3A. Different solutions (25 µL) with food dye was added in the circular zone and the optical micrographs were obtained 20 min later. The micrographs were presented in Figure 3B and indicated that the paint barrier exhibited the high chemical resistance towards the various kinds of chemicals such as acid and alkaline solutions, organic solvents, surfactants, buffer solution and the reducing reagent.

The microzone assay performance for iron

The microzone array consisted of 9 zones arranged into 3 columns and 3 rows. To investigate the capability of the developed device, iron was used as the model analyte. The sp-µPADs for iron assay was feasible and the optimized parameter was obtained experimentally. The results shown in Figure S1 (Supplementary Information (SI) section) indicated that the B channel was selected as
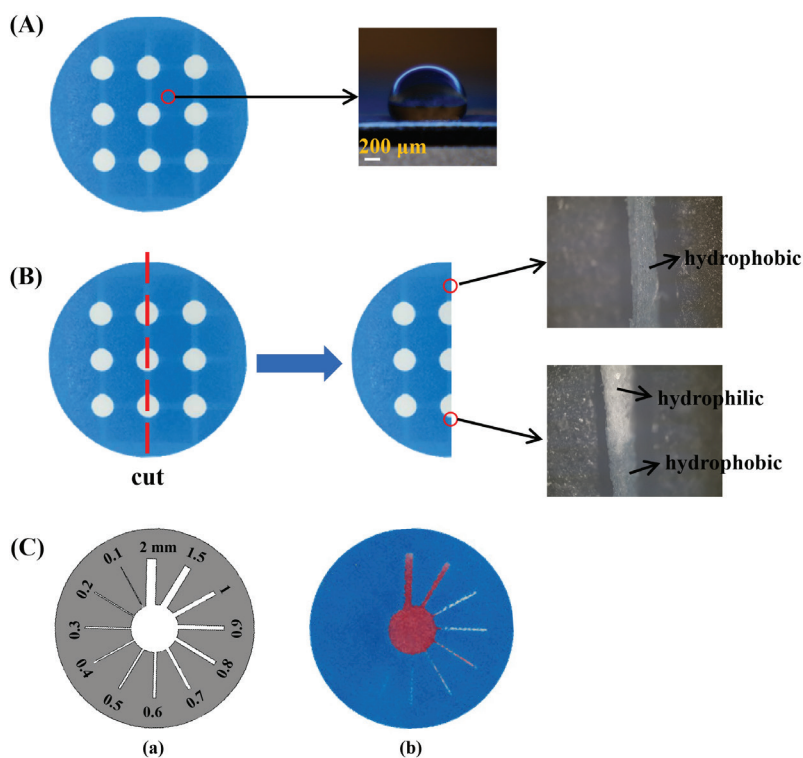

Figure 2. (A) The picture obtained after the water droplet was dropped on the surface of the sp-µPADs. (B) The cross section of the sp-µPADs captured under an optical microscope at 225× magnification. (C) The design of the device for the channel size calibration (a) and the fabricated device treated with the red food dye (b).
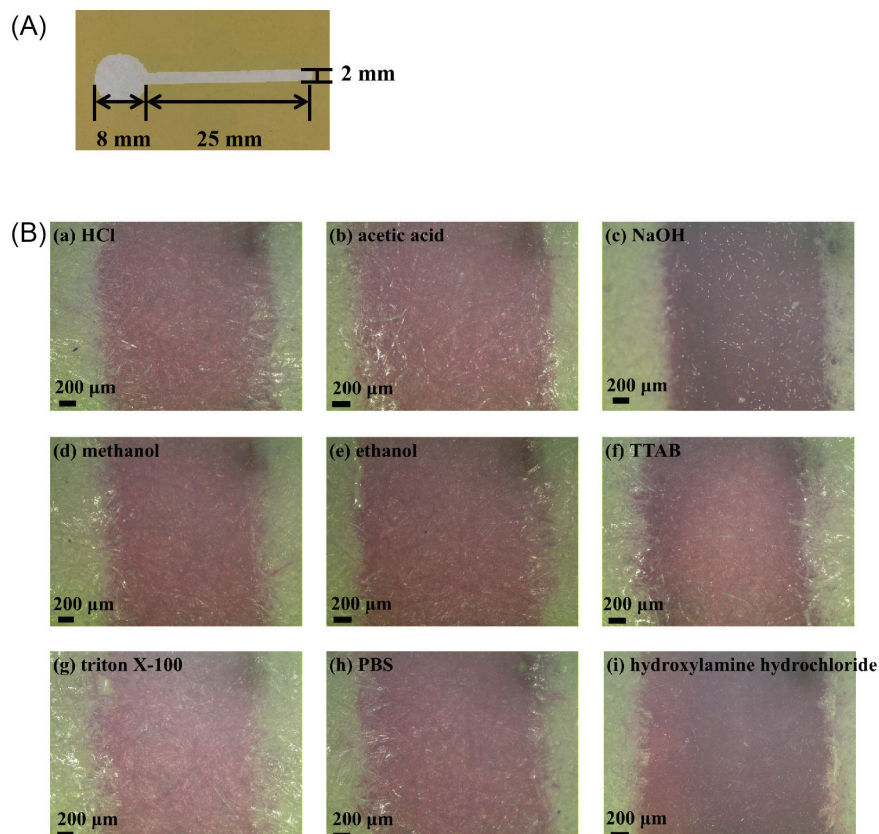
Figure 3. (A) The fabricated distance-based sp-µPADs. (B) The optical micrographs of the paint barrier after adding different solutions: (a) 150 mmol L^{-1} hydrochloric acid, (b) 150 mmol L^{-1} acetic acid, (c) 150 mmol L^{-1} sodium hydroxide, (d) 50% (v/v) methanol, (e) 50% (v/v) ethanol, (f) 5% (m/v) tetradecyltrimethylammonium bromide (TTAB), (g) 5% (m/v) triton X-100, (h) phosphate buffer solution (PBS) (100 mmol L^{-1} pH 7.4), (i) 150 mmol L^{-1} hydroxylamine hydrochloride.

the analytical signal due to its high sensitivity. The results in Figure S2 (SI section) indicated that 100 mmol L^{-1} was the optimized concentration of phen for iron assay. Under the optimized conditions, a series of Fe^{III} standards were pipetted into the microzones. The assay color intensity was analyzed using ImageJ software.[40] It is noted from Figure 4a that the color in the assay zone gradually darken with the concentrations of Fe^{III} increasing from 0 to 400 mg L^{-1}, resulting in a notable decrease in the blue channel intensity. Figure 4b shows that a strong linear calibration plot (blue channel intensity = $-0.7235C_{Fe} + 202$, $R^2 = 0.9951$) was obtained with a linear range from 5 to 150 mg L^{-1}. The limit of detection (LOD) was calculated to be 2.2 mg L^{-1} by $3\sigma/S$, σ is the standard deviation of the signal in nine parallel blank measurements and S is the slope of the calibration equation. For comparison, some representative chemosensors for iron detection are summarized in Table 1. It is noted that the performance of the sp-µPADs in this work were comparable with most of the literature listed in Table 1. The µPADs fabricated by Henry and co-workers[54,55] presented the lower LOD for iron assay using the same reaction. The possible reason is that the poly(acrylic acid) and polyethylene glycol were added to immobilize the

colored product and increase the hydrophilicity in the reservoir, resulting in the better assay performance.

To investigate the anti-interference ability of the fabricated sp-µPADs, the selectivity experiment was carried out using several common interferent ions as the interferents (Ca^{II}, Co^{II}, K^{I}, Mg^{II}, Na^{I}, Ni^{II}, Pb^{II}, Zn^{II}). Figure S3 (SI section) shows the images and the color values in the B channel of the assay zones with different ions. With a comparison to the blank, Fe^{III} solution (100 mg L^{-1}) produced an orange-red color in the detection zone and resulted in a significant decrease of the color intensity. The other ions (10000 mg L^{-1}) produced no color with the reagent. The color intensities obtained in the interferents were almost the same as the intensity obtained in the blank, demonstrating the good selectivity of the sp-µPADs for Fe^{III} detection. The repeatability was investigated by performing the determination of five concentration levels (5, 30, 50, 100, 150 mg L^{-1}) with nine replicate measurements using the sp-µPADs. For the five concentration levels investigated, the relative standard deviations (RSD) were 4.6, 4.5, 3.6, 3.5 and 4.8%, respectively. The results demonstrated that the developed sp-µPADs performed a satisfactory repeatability.

Table 1. The performance contrast of the different chemosensors for iron detection

Sensing reagents/materials	Method	Linear range / (mg L^{-1})	LOD / (mg L^{-1})	Reference
Compound **2**[a]	fluorescence		2.4	50
Gold nanoparticles and acidic thiourea mixture	colorimetric	100-500	50	51
Bathophenanthroline[b]	colorimetric	3.3-470	3.3	48
Bathophenanthroline[b]	colorimetric	20-1300	20	48
Sensor 5[c]	fluorescence		5.2	52
Phen	colorimetric	5-125		53
Phen	colorimetric	5-150	2.2	this work

[a]3-(4-(Dimethylamino)phenyl)-1-(5-methyl-1-(naphthalen-1-yl)-1*H*-1,2,3-triazol-4-yl)prop-2-en-1-one; [b]4,7-diphenyl-1-1,10-phenanthroline; [c]5-ethoxycarbonyl-6-methyl-4-phenyl-2-[(7-chloroquinolin-4-ylamino)butylamino]pyrimidine. LOD: limit of detection; phen: 1,10-phenanthroline monohydrate.
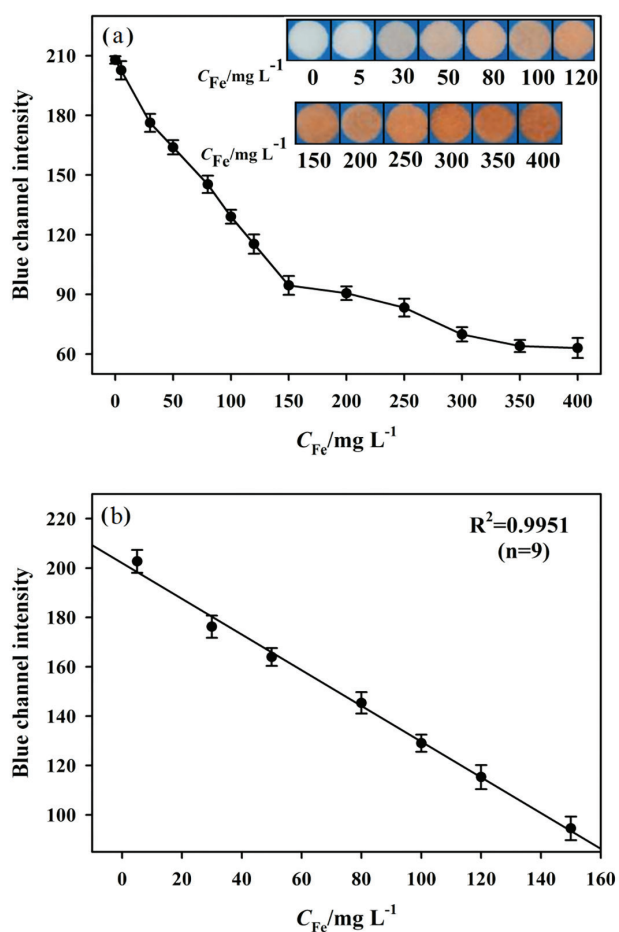

Figure 4. (a) The results for iron assay. Inset: the pictures of the microzones after adding a series of Fe^{III} standards. (b) Calibration curve for iron assay.

To study the practicability of the sp-μPADs for iron assay, the recovery test was performed using the drinking water as the real world sample. Iron was not detected in the drinking water by our method. The possible reason may be that the concentration of iron in the sample was below the LOD, or there was no iron in the water sample. The water sample was spiked with the standard solutions

of Fe^{III}. The results of applying the assay to the real world sample are listed in Table S1 (SI section). The recoveries of Fe^{III} ranged from 94.0 to 108.8%. In addition, all the RSD values of the recovery test were found to be below 4%, showing that the sp-μPADs were suitable for iron assay in the real world sample.

The simultaneous assay of copper and nickel

The applicability was also demonstrated by the simultaneous assay of copper and nickel. The assay reagents for the two ions assay were described in the "The multiplexed assay of eight analytes" sub-section. The fabricated device for this experiment was designed with two assay zones on both sides and one sample introduction zone in the center. All the circular zones in the device were designed with a diameter of 6 mm. The size of the channels between the circular zones was 5.4 mm (length) × 2 mm (width). 1.8 μL of the reagents were added in the assay zones on both sides and dried at RT for 10 min. 20 μL of the standard was then added to the circular zone in the center. The photos of the sp-μPADs were captured 10 min later and the color intensity was analyzed by the free image processing software. It is noted from Figure 5 that when the concentrations of the analytes increased, the colors in the assay zones became darker, indicating that more complexation between the analyte and reagents was produced. The linear range was 5-9 mmol L^{-1} for the copper assay and 1-6 mmol L^{-1} for the nickel assay, respectively. The detectable limit was 5 mmol L^{-1} for the copper assay and 1 mmol L^{-1} for the nickel assay, respectively. The results demonstrated that the sp-μPADs were successfully fabricated and could be extended to the simultaneous assay of two analytes.

The distance-based sp-μPADs for the detection of BSA

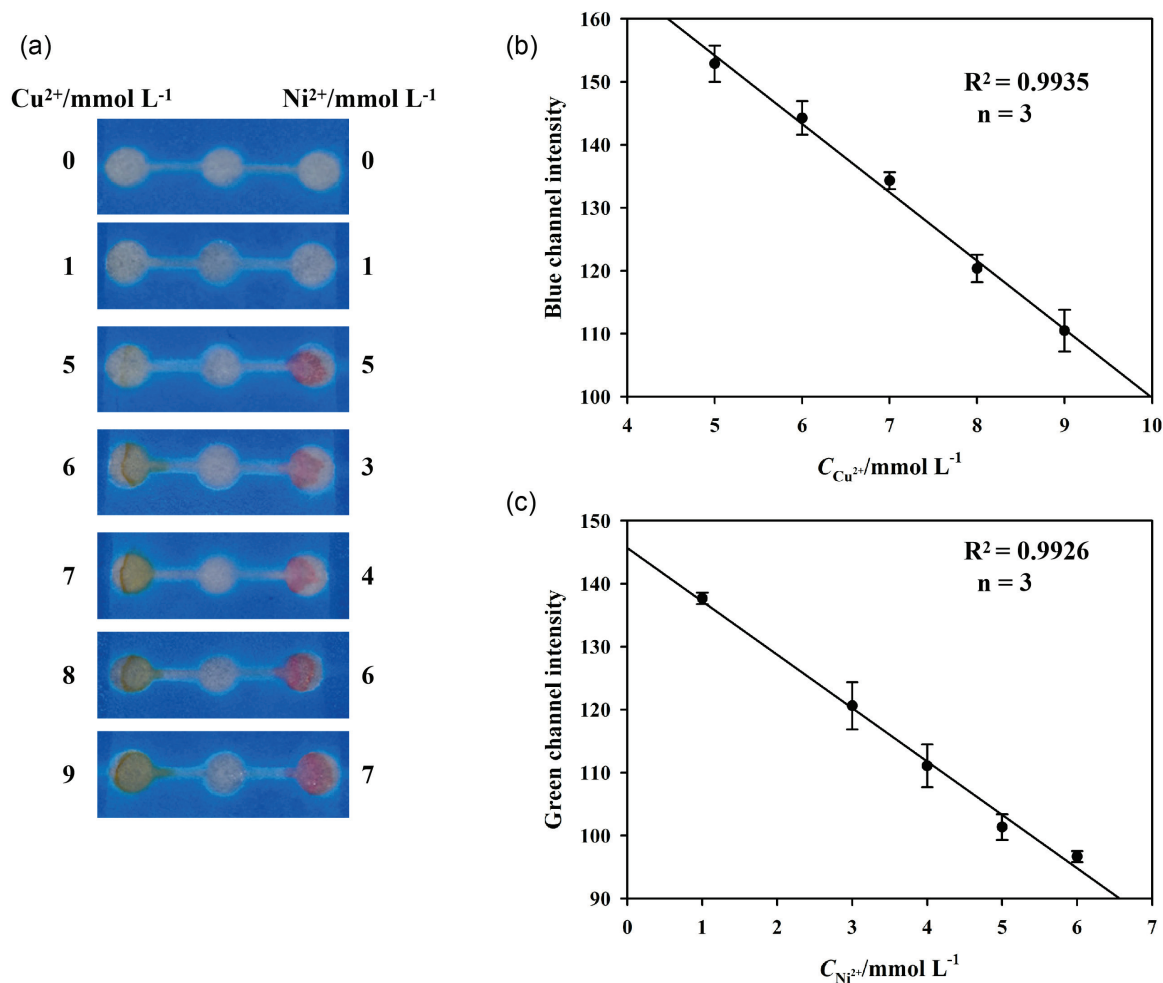The distance-based sp-μPADs were also prepared by

Figure 5. (a) The photos of the sp-μPADs for the simultaneous assay of copper and nickel. (b) The calibration curve for copper assay. (c) The calibration curve for nickel assay.

the paint spraying method, consisting of a circular reservoir with a radius of 4 mm for analyte introduction and a straight channel (2×25 mm) for the distance measurement. BSA was used as the model analyte to prove the applicability of the distance-based sp-μPADs. For the detection of BSA, the reagents including 250 mmol L^{-1} citric acid and 3 mmol L^{-1} TBPB were dissolved in 95% (v/v) ethanol. Then, 3 μL of the reagents were pipetted into the straight channel and dried at RT for 10 min. 25 μL of BSA standard was then added to the circular zone. After 5 min of reaction, the color distance was measured. The photos of the distance-based sp-μPADs for BSA assay are presented in the Figure 6a. The color of the reagents were yellow but produced a dark blue product that was easily visible after the reaction with BSA. Moreover, when the concentration of BSA increased, the color distance rose higher and higher, indicating a positive correlation between them. It is noted from Figure 6b that the linear range for BSA assay was 0.05-1 g L^{-1} and the visual limit of detection was 0.05 g L^{-1}. The linearity for the detection of BSA was expressed by the squared correlation

coefficient (R^2), which equaled 0.9881. Although the first data point (0.05 g L^{-1}, 1.7250 mm) reduces the correlation between the set of data, it was not removed. The reason is that the urinary albumin excretion (i.e., microalbuminuria) is an important marker for the early-stage renal failure when the levels of urine albumin are between 0.02 and 0.2 g L^{-1}.[56] Therefore, the distance assay of BSA sacrifices the linearity for the wide dynamic range, which partially overlaps the clinical range of urine albumin. The results demonstrated that the distance-based sp-μPADs were successfully fabricated by the paint spraying technique and exhibited a promising prospect for bioassay.

The flower-shaped sp-μPADs fabricated by the paint-spraying method for the multiplexed assay

More complex design was employed for the device fabrication. The layout of the flower shaped sp-μPADs were manufactured with the spraying parameters listed as follows: the channel with a 2.0 mm width and a 4.5 mm length, the
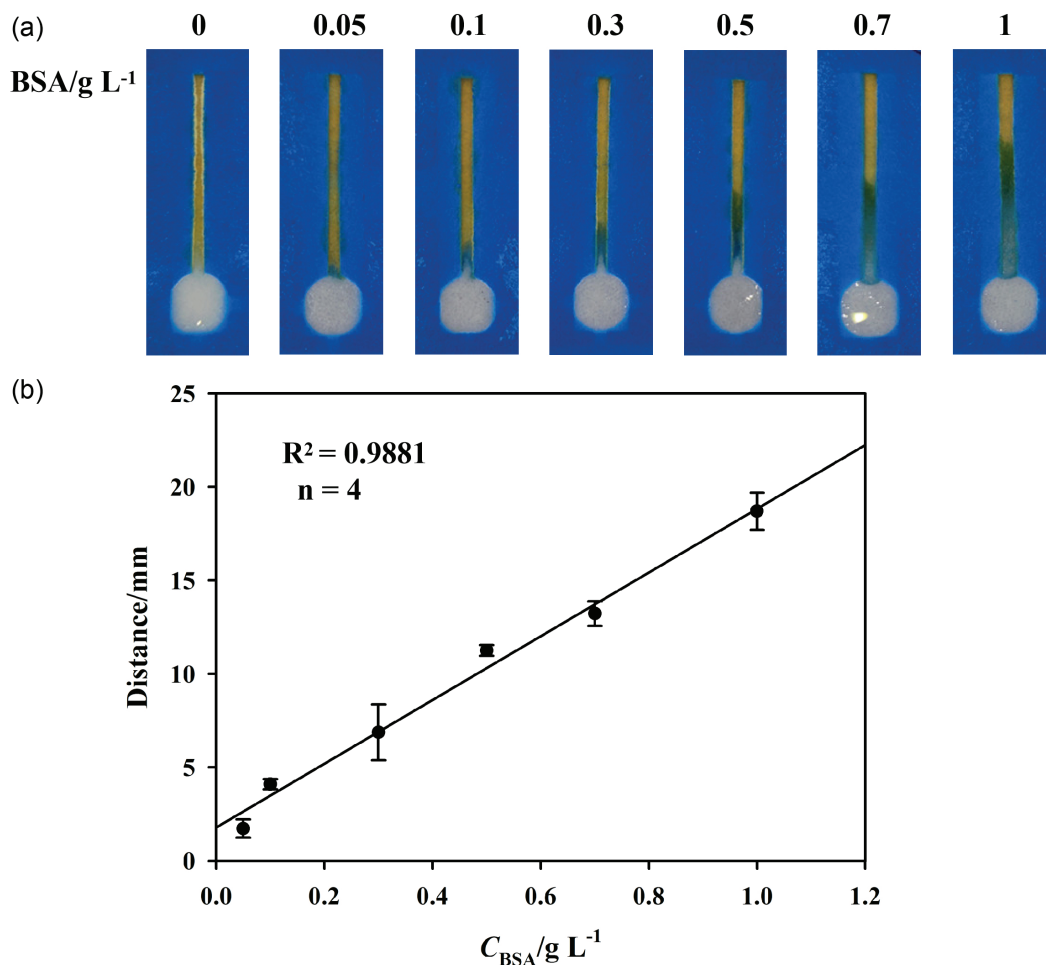
Figure 6. (a) The photos of the fabricated distance-based sp-µPADs for BSA assay. (b) The calibration curve for BSA assay.

central analyte introduction reservoir with a diameter of 6.0 mm, the outer circular assay zone with a diameter of 4.0 mm. Figure 7 shows a photograph of the flower-shaped sp-µPADs for simultaneously detecting a model mixture containing the eight analytes including BSA (1 g L^{-1}), glucose (2 mmol L^{-1}), nitrite (1 mmol L^{-1}), thiocyanate (10 mmol L^{-1}), lactate (20 mmol L^{-1}), pH (7), Cu^{II} (20 mmol L^{-1}) and Ni^{II} (20 mmol L^{-1}). These analytes are clinically relevant and commonly measured in biological systems such as urine or saliva, and their values are closely related to the human health. With a comparison to the blank, the eight analytes were successfully detected at the same time. Therefore, certain diseases could be quickly screened by the color changes obtained in the developed flower shaped sp-µPADs, providing a great analytical platform for the clinical testing.

Conclusions

The simple, low-cost sp-µPADs have been fabricated by the paint spraying technique with simple or complex designs by changing the patterned PMMA mask. The
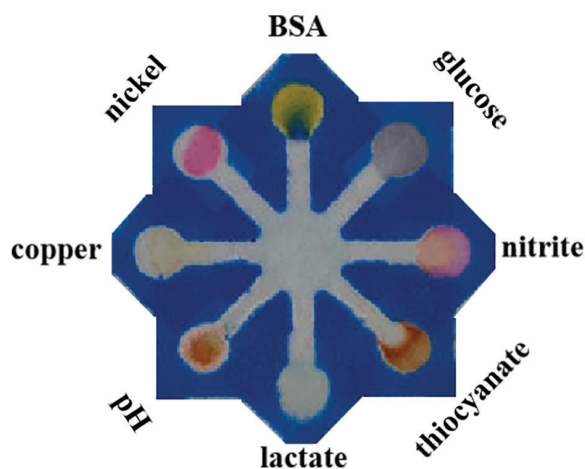

Figure 7. The photograph of the flower-shaped sp-µPADs for the multiplexed assay of a model mixture with a volume of 15 µL: BSA (1 g L^{-1}), glucose (2 mmol L^{-1}), nitrite (1 mmol L^{-1}), thiocyanate (10 mmol L^{-1}), lactate (20 mmol L^{-1}), pH (7), Cu^{II} (20 mmol L^{-1}) and Ni^{II} (20 mmol L^{-1}).

applicability of the sp-µPADs was proved by implementing colorimetric detections of one or more analytes. The microzone assay performance for iron exhibited a LOD of

2.2 mg L^{-1} and a linear range of 5-150 mg L^{-1}. The detectable limits for the simultaneous assay of copper and nickel were 5 mmol L^{-1} for copper assay and 1 mmol L^{-1} for nickel assay, respectively. The distance-based sp-µPADs were successfully fabricated and applied for the detection of BSA with a visual limit of detection of 0.05 g L^{-1}. Furthermore, the possible application of the flower-shaped sp-µPADs were demonstrated by the multiplexed assay of eight analytes. Accordingly, the sp-µPADs offered a promising prospect on detecting single analyte or multiple analytes, showing the potential applications in environmental analysis and bioassays.

Supplementary Information

Supplementary information is available free of charge at http://jbcs.sbq.org.br as PDF file.

Acknowledgments

Author Contributions

B. N., S. Z. and M. D. carried out the experiments and their contributions to the paper were equal. P. Y. designed the µPADs, searched the references, and wrote the manuscript. Y. Y. collected the pictures of devices under the optical microscope and contributed to the manuscript edition. W. L. and L. Y. interpreted the data and edited the manuscript.

References

1. Martinez, A. W.; Phillips, S. T.; Butte, M. J.; Whitesides, G. M.; *Angew. Chem., Int. Ed.* **2007**, *46*, 1318.

2. Channon, R. B.; Nguyen, M. P.; Scorzelli, A. G.; Henry, E. M.; Volckens, J.; Dandy, D. S.; Henry, C. S.; *Lab Chip* **2018**, *18*, 793.

3. Jiang, Y.; Wang, P. C.; Locascio, L. E.; Lee, C. S.; *Anal. Chem.* **2001**, *73*, 2048.

4. Lee, J.; Soper, S. A.; Murray, K. K.; *J. Mass Spectrom.* **2009**, *44*, 579.

5. Nie, Z.; Nijhuis, C. A.; Gong, J.; Chen, X.; Kumachev, A.; Martinez, A. W.; Narovlyansky, M.; Whitesides, G. M.; *Lab Chip* **2010**, *10*, 477.

6. Sun, X.; Wang, H.; Jian, Y.; Lan, F.; Zhang, L.; Liu, H.; Ge, S.; Yu, J.; *Biosens. Bioelectron.* **2018**, *105*, 218.

7. Hassani, A.; Skorobogatiy, M.; *Opt. Express* **2006**, *14*, 11616.

8. Malic, L.; Veres, T.; Tabrizian, M.; *Biosens. Bioelectron.* **2009**, *24*, 2218.

9. Wang, L.; Musile, G.; McCord, B. R.; *Electrophoresis* **2018**, *39*, 470.

10. Ellerbee, A. K.; Phillips, S. T.; Siegel, A. C.; Mirica, K. A.; Martinez, A. W.; Striehl, P.; Jain, N.; Prentiss, M.; Whitesides, G. M.; *Anal. Chem.* **2009**, *81*, 8447.

11. Li, B.; Fu, L.; Zhang, W.; Feng, W.; Chen, L.; *Electrophoresis* **2014**, *35*, 1152.

12. Fiedoruk-Pogrebniak, M.; Granica, M.; Koncki, R.; *Talanta* **2018**, *178*, 31.

13. Weng, X.; Neethirajan, S.; *Microchim. Acta* **2017**, *184*, 4545.

14. Qi, J.; Li, B.; Wang, X.; Fu, L.; Luo, L.; Chen, L.; *Anal. Chem.* **2018**, *90*, 11827.

15. Coltro, W. K. T.; de Jesus, D. P.; da Silva, J. A. F.; do Lago, C. L.; Carrilho, E.; *Electrophoresis* **2010**, *31*, 2487.

16. Lisowski, P.; Zarzycki, P. K.; *Chromatographia* **2013**, *76*, 1201.

17. Caputo, D.; de Cesare, G.; Dolci, L. S.; Mirasoli, M.; Nascetti, A.; Roda, A.; Scipinotti, R.; *IEEE Sens. J.* **2013**, *13*, 2595.

18. Kamruzzaman, M.; Alam, A. M.; Kim, K. M.; Lee, S. H.; Kim, Y. H.; Kabir, A. H.; Kim, G. M.; Dang, T. D.; *Biomed. Microdevices* **2013**, *15*, 195.

19. Koesdjojo, M. T.; Pengpumkiat, S.; Wu, Y.; Boonloed, A.; Huynh, D.; Remcho, T. P.; Remcho, V. T.; *J. Chem. Educ.* **2015**, *92*, 737.

20. Rossini, E. L.; Milani, M. I.; Carrilho, E.; Pezza, L.; Pezza, H. R.; *Anal. Chim. Acta* **2018**, *997*, 16.

21. Chabaud, K. R.; Thomas, J. L.; Torres, M. N.; Oliveira, S.; McCord, B. R.; *Forensic Chem.* **2018**, *9*, 35.

22. Taghizadeh-Behbahani, M.; Hemmateenejad, B.; Shamsipur, M.; *Chem. Pap.* **2018**, *72*, 1239.

23. Liu, C.; Gomez, F. A.; Miao, Y.; Cui, P.; Lee, W.; *Talanta* **2019**, *194*, 171.

24. da Silva, G. O.; de Araujo, W. R.; Paixão, T. R.; *Talanta* **2018**, *176*, 674.

25. Cao, R.; Zhang, X.; Tan, W.; Shen, W.; *Cellulose* **2018**, *25*, 583.

26. Asano, H.; Shiraishi, Y.; *Anal. Chim. Acta* **2015**, *883*, 55.

27. Abdollahi-Aghdam, A.; Majidi, M. R.; Omidi, Y.; *BioImpacts* **2018**, *8*, 237.

28. Puneeth, S. B.; Goel, S.; *IEEE Trans. Electron Devices* **2019**, *66*, 3196.

29. Chiang, C. K.; Kurniawan, A.; Kao, C. Y.; Wang, M. J.; *Talanta* **2019**, *194*, 837.

30. Zhang, H.; Smith, E.; Zhang, W.; Zhou, A.; *Biomed. Microdevices* **2019**, *21*, 48.

31. Casto, L. D.; Schuster, J. A.; Neice, C. D.; Baker, C. A.; *Anal. Methods* **2018**, *10*, 3616.

32. Cardoso, T. M.; Garcia, P. T.; Coltro, W. K.; *Anal. Methods* **2015**, *7*, 7311.

33. Pena-Pereira, F.; Lavilla, I.; Bendicho, C.; *Talanta* **2016**, *147*, 390.

34. Atabakhsh, S.; Ashtiani, S. J.; *Microfluid. Nanofluid.* **2019**, *23*, 69.

35. Al-Qadiri, H. M.; Ovissipour, M.; Al-Alami, N.; Govindan, B. N.; Shiroodi, S. G.; Rasco, B.; *J. Food Sci.* **2016**, *81*, M1177.

36. Cardoso, T. M. G.; de Souza, F. R.; Garcia, P. T.; Rabelo, D.; Henry, C. S.; Coltro, W. K. T.; *Anal. Chim. Acta* **2017**, *974*, 63.

37. Nurak, T.; Praphairaksit, N.; Chailapakul, O.; *Talanta* **2013**, *114*, 291.

38. Hu, R. G.; Zhang, S.; Bu, J. F.; Lin, C. J.; Song, G. L.; *Prog. Org. Coat.* **2012**, *73*, 129.

39. *ZWCAD*, v.18.0.55.0; Guangzhou Zhongwang Longteng Software Co., Ltd., China, 2018.

40. *ImageJ*, v.1.50b; National Institutes of Health, USA, 2017.

41. Gammella, E.; Recalcati, S.; Rybinska, I.; Buratti, P.; Cairo, G.; *Oxid. Med. Cell. Longevity* **2015**, *2015*, 230182.

42. Kontoghiorghe, C. N.; Kontoghiorghes, G. J.; *World J. Methodol.* **2016**, *6*, 1.

43. Garcia, P. T.; Cardoso, T. M. G.; Garcia, C. D.; Carrilho, E.; Coltro, W. K. T.; *RSC Adv.* **2014**, *4*, 37637.

44. Yu, P.; Deng, M.; Yang, Y.; *Sensors* **2019**, *19*, 4082.

45. Dungchai, W.; Chailapakul, O.; Henry, C. S.; *Anal. Chim. Acta* **2010**, *674*, 227.

46. Koh, A.; Kang, D.; Xue, Y.; Lee, S.; Pielak, R. M.; Kim, J.; Hwang, T.; Min, S.; Banks, A.; Bastien, P.; Manco, M. C.; Wang, L.; Ammann, K. R.; Jang, K. I.; Won, P.; Han, S.; Ghaffari, R.; Paik, U.; Slepian, M. J.; Balooch, G.; Huang, Y.; Rogers, J. A.; *Sci. Transl. Med.* **2016**, *8*, 366ra165.

47. Xie, G. L.; Yu, H.; Deng, M. H.; Zhao, X. L.; Yu, P.; *Chem. Pap.* **2019**, *73*, 1509.

48. Cate, D. M.; Noblitt, S. D.; Volckens, J.; Henry, C. S.; *Lab Chip* **2015**, *15*, 2808.

49. Lim, W. Y.; Goh, B. T.; Khor, S. M.; *J. Chromatogr. B* **2017**, *1060*, 424.

50. Singh, H.; Sindhu, J.; Khurana, J. M.; *Sens. Actuators, B* **2014**, *192*, 536.

51. Tripathy, S. K.; Woo, J. Y.; Han, C. S.; *Sens. Actuators, B* **2013**, *181*, 114.

52. Kaur, P.; Kaur, H.; Singh, K.; *RSC Adv.* **2013**, *3*, 64.

53. Apilux, A.; Dungchai, W.; Siangproh, W.; Praphairaksit, N.; Henry, C. S.; Chailapakul, O.; *Anal. Chem.* **2010**, *82*, 1727.

54. Mentele, M. M.; Cunningham, J.; Koehler, K.; Volckens, J.; Henry, C. S.; *Anal. Chem.* **2012**, *84*, 4474.

55. Rattanarat, P.; Dungchai, W.; Cate, D.; Volckens, J.; Chailapakul, O.; Henry, C. S.; *Anal. Chem.* **2014**, *86*, 3555.

56. Martinez, A. W.; Phillips, S. T.; Carrilho, E.; Thomas, S. W.; Sindi, H.; Whitesides, G. M.; *Anal. Chem.* **2008**, *80*, 3699.